

Supplementary Information

Solid-State Synthesis of $\text{Si}_{1-x}\text{Ge}_x$ Nanoalloys with Composition-Tunable Energy Gaps and Visible to Near Infrared Optical Properties

Griffin C. Spence,¹ David S. Pate,² Corentin Villot,¹ Roshana M. Fouzie,¹ Lisa S. Graves,¹

Ka Un Lao,¹ Ümit Özgür,² and Indika U. Arachchige,^{1,}*

¹Department of Chemistry, Virginia Commonwealth University, Richmond, Virginia 23284-
2006, United States

²Department of Electrical and Computer Engineering, Virginia Commonwealth University,
Richmond, Virginia 23284-9052, United States

Email: iuarachchige@vcu.edu

Table S1. Absorption onsets of Si_{1-x}Ge_x alloy NCs (x = 0 – 14.4%) obtained from indirect-gap Tauc analysis in the lower energy region along with lattice parameters and d-spacing values obtained from PXRD, SAED, and HRTEM studies.

Experimental Composition	Tauc Indirect (E_g^{i2})	Lattice Parameter (Å)	d-spacing, XRD (Å)	d-spacing, TEM (Å)	d-spacing, SAED (Å)
Si _{1.000} Ge _{0.000}	1.16	5.4361	3.14	3.12	3.12
Si _{0.988} Ge _{0.012}	1.15	5.4436	3.15	3.11	3.13
Si _{0.957} Ge _{0.043}	1.12	5.4475	3.15	3.12	3.14
Si _{0.944} Ge _{0.056}	1.12	5.4491	3.16	3.13	3.15
Si _{0.914} Ge _{0.086}	1.10	5.4587	3.16	3.13	3.15
Si _{0.884} Ge _{0.116}	1.22	5.4624	3.16	3.14	3.16
Si _{0.856} Ge _{0.144}	1.00	5.4711	3.17	3.14	3.16

Table S2. Experimental parameters used in the synthesis of Si and Si_{1-x}Ge_x alloy NCs.

Nominal Composition	Exp. Si, %	Exp. Ge, %	Mass of GeI₂ (g)	Etching Time (h)
Si _{1.000} Ge _{0.000}	100	0	0	1
Si _{0.950} Ge _{0.050}	98.79	1.21	0.240	16
Si _{0.935} Ge _{0.065}	95.75	4.25	0.328	24
Si _{0.920} Ge _{0.080}	94.36	5.64	0.404	24
Si _{0.850} Ge _{0.150}	91.56	8.44	0.717	48
Si _{0.800} Ge _{0.200}	88.48	11.62	0.960	48
Si _{0.700} Ge _{0.300}	85.57	14.43	1.434	48
Si _{0.600} Ge _{0.400}	70.03	29.70	1.914	48

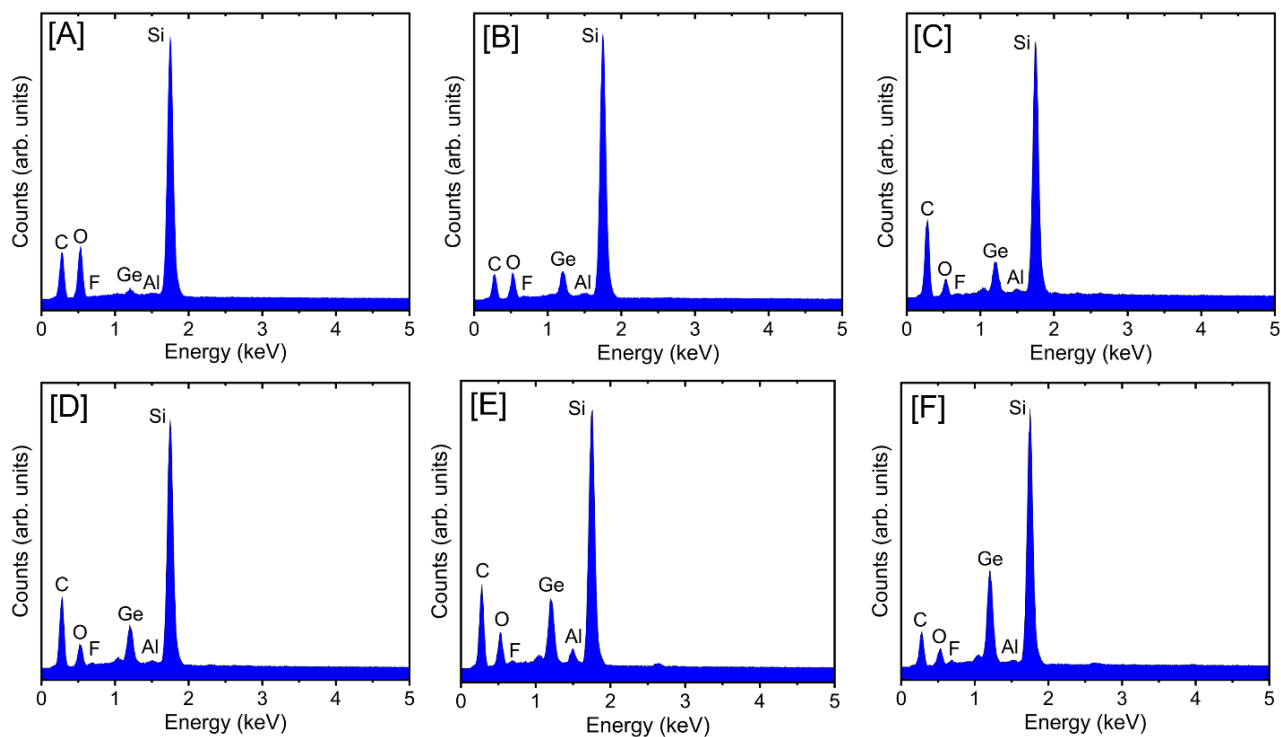


Figure S1. Representative SEM-EDS spectra of [A] $\text{Si}_{0.988}\text{Ge}_{0.012}$, [B] $\text{Si}_{0.957}\text{Ge}_{0.043}$, [C] $\text{Si}_{0.944}\text{Ge}_{0.056}$, [D] $\text{Si}_{0.916}\text{Ge}_{0.084}$, [E] $\text{Si}_{0.884}\text{Ge}_{0.116}$, and [F] $\text{Si}_{0.856}\text{Ge}_{0.144}$ alloy NCs. Carbon originates from dodecyl ligands and carbon tape used to retain the $\text{Si}_{1-x}\text{Ge}_x$ NCs on the sample holder. Oxygen and aluminum originate from the sample holder. Fluorine originates from Si-F ligands from etching.

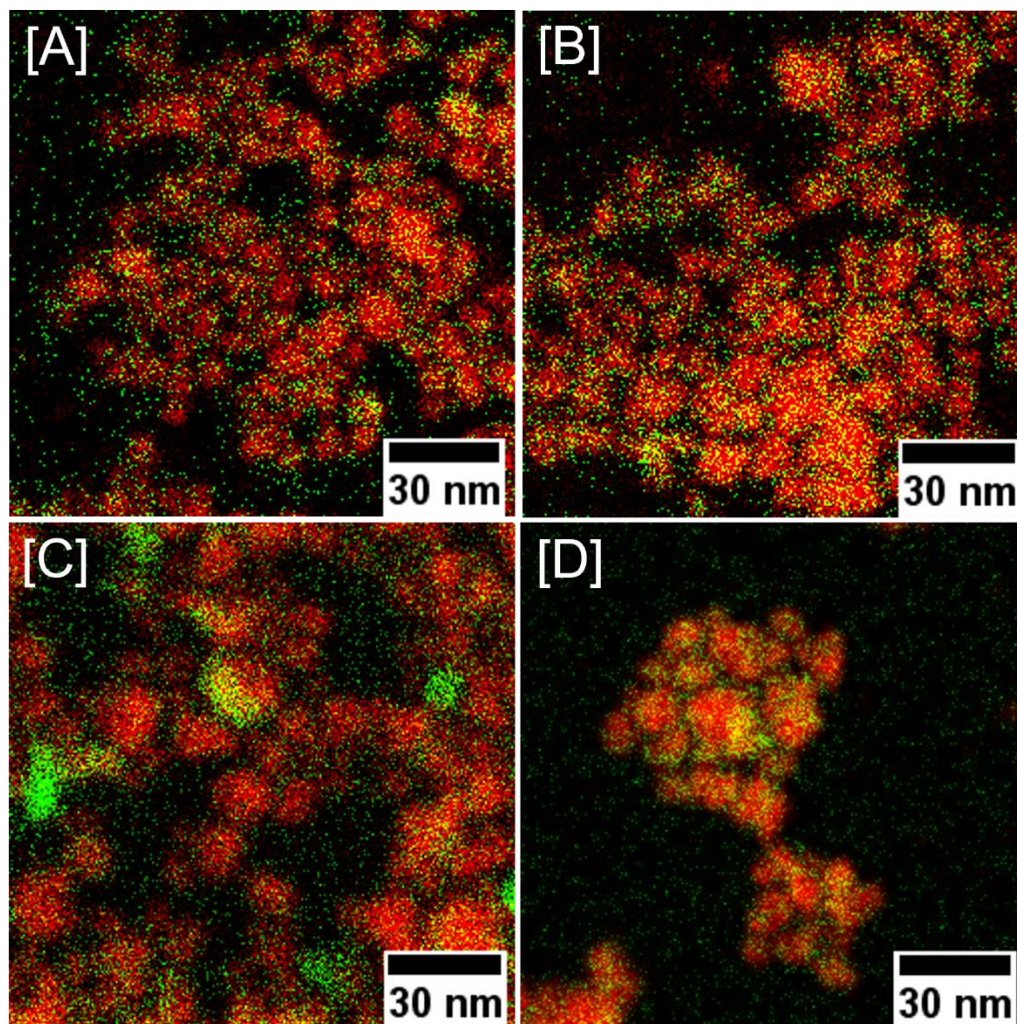


Figure S2. STEM-HAADF elemental map overlays of Si (red) and Ge (green) for [A] $\text{Si}_{0.915}\text{Ge}_{0.085}$ NCs produced at 600 °C for 1 h, [B] $\text{Si}_{0.905}\text{Ge}_{0.095}$ NCs produced at 600 °C for 4 h, [C] $\text{Si}_{0.913}\text{Ge}_{0.087}$ NCs produced at 600 °C for 7 h, and [D] $\text{Si}_{0.864}\text{Ge}_{0.137}$ NCs produced at 800 °C for 3 h.

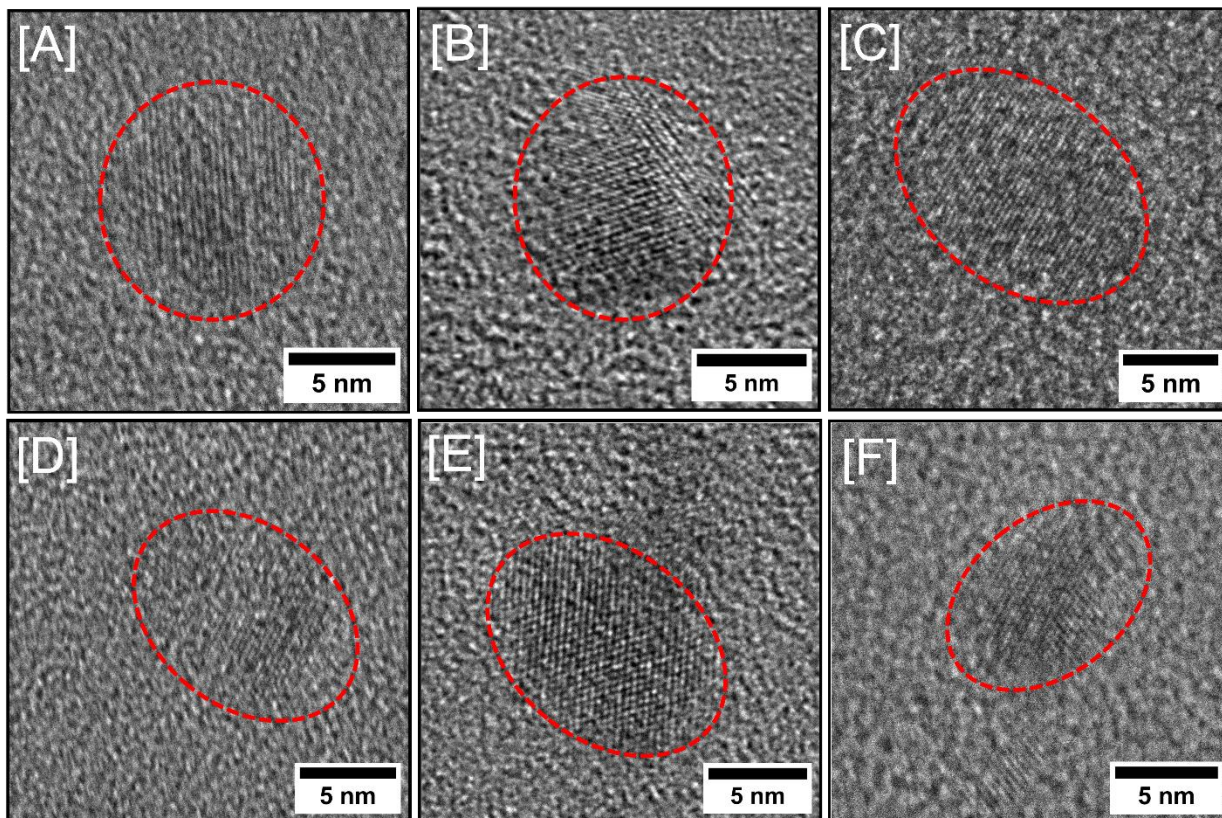


Figure S3. Representative HRTEM images of [A] $\text{Si}_{0.988}\text{Ge}_{0.012}$, [B] $\text{Si}_{0.957}\text{Ge}_{0.043}$, [C] $\text{Si}_{0.944}\text{Ge}_{0.056}$, [D] $\text{Si}_{0.916}\text{Ge}_{0.084}$, [E] $\text{Si}_{0.884}\text{Ge}_{0.116}$, and [F] $\text{Si}_{0.856}\text{Ge}_{0.144}$ alloy NCs displaying lattice fringes. Red dashed ovals/circles represent particle shape for clarity.

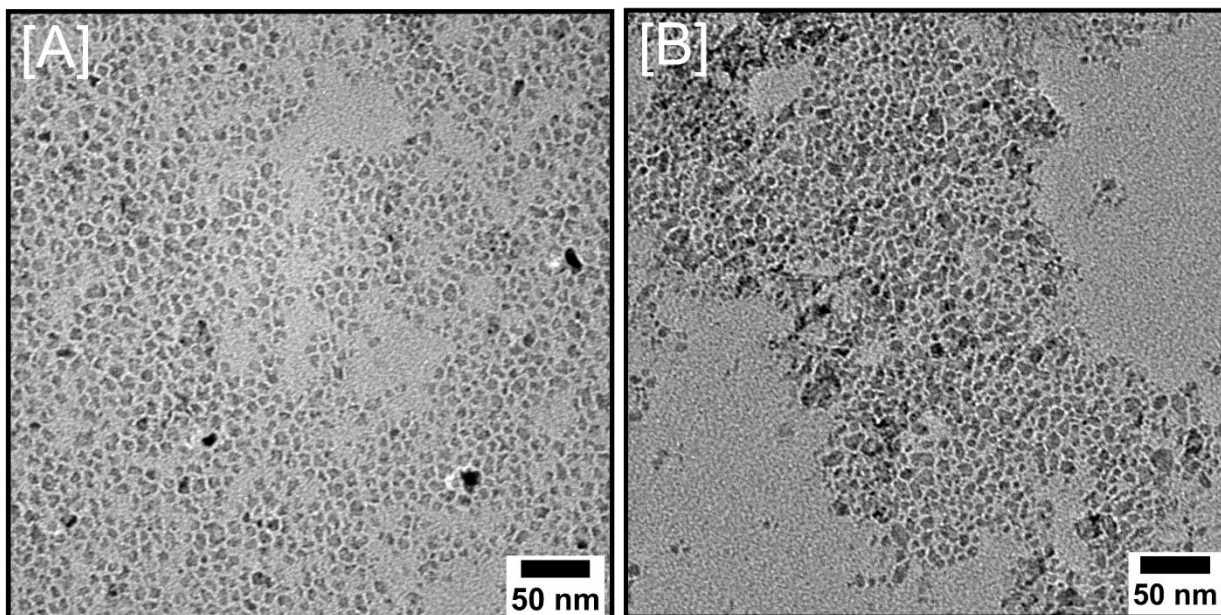


Figure S4. Representative TEM images of [A] $\text{Si}_{0.944}\text{Ge}_{0.056}$, [B] $\text{Si}_{0.856}\text{Ge}_{0.144}$ alloy NCs.

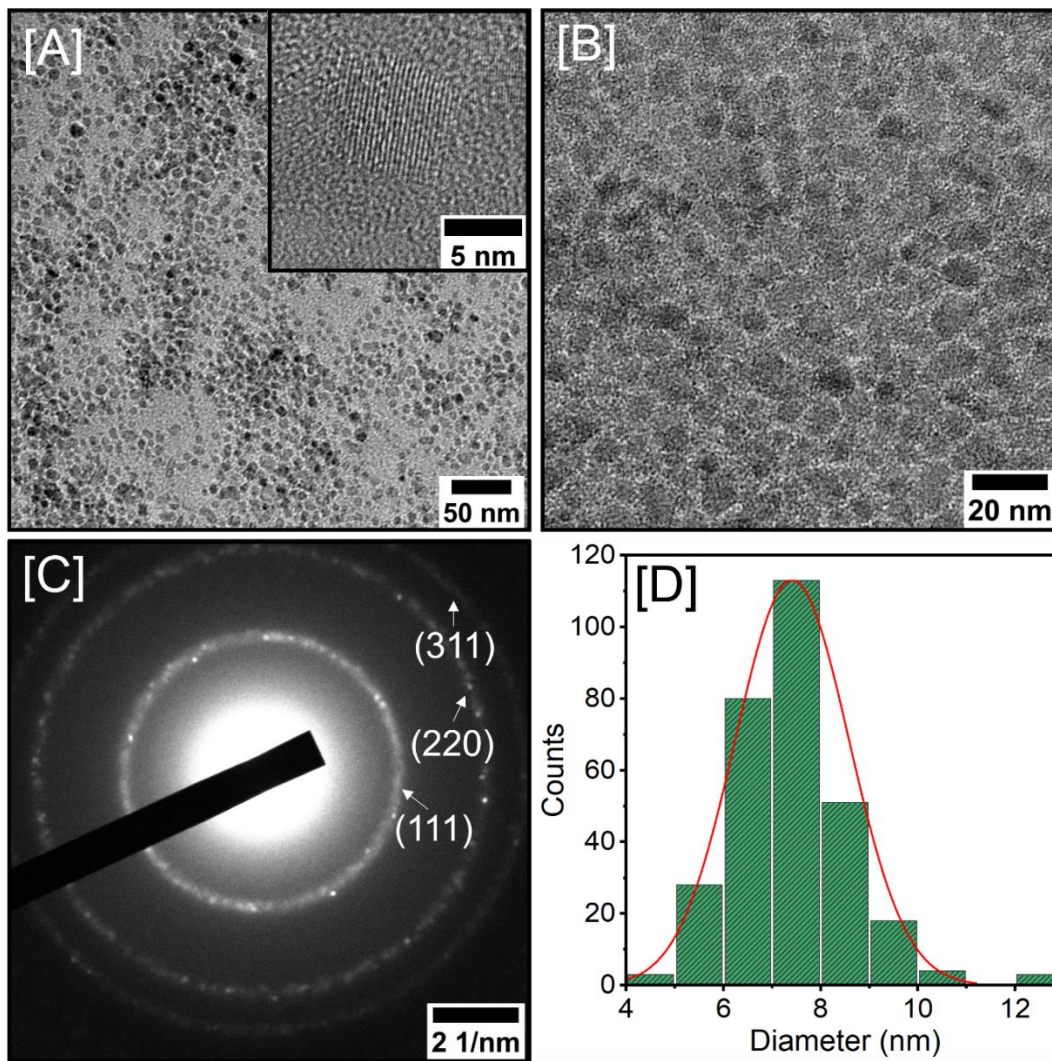


Figure S5. Representative [A-B] LRTEM images and [C] a SAED pattern of Si NCs produced at 1100 °C for 4 h. The inset in A shows a HRTEM image of a single particle. [D] Size histogram of Si NCs shown in [A].

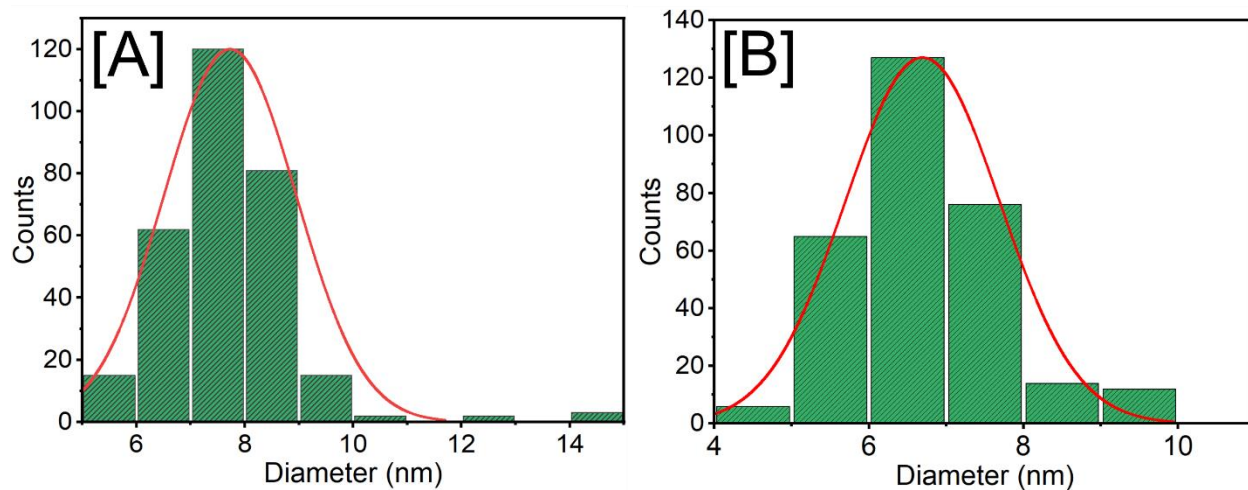


Figure S6. Size histograms of [A] $\text{Si}_{0.944}\text{Ge}_{0.056}$ and [B] $\text{Si}_{0.856}\text{Ge}_{0.144}$ alloy NCs shown in Figure S4A and B, respectively.

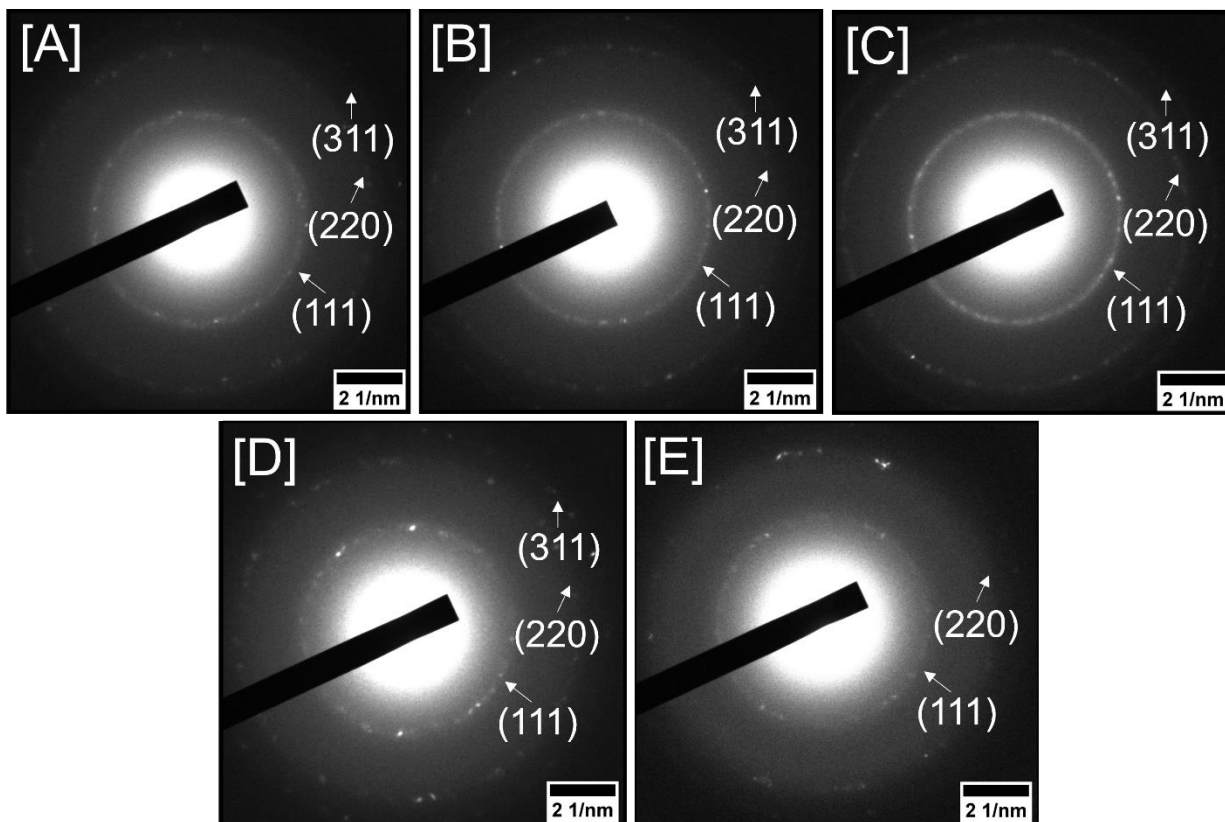


Figure S7. Representative SAED patterns of [A] $\text{Si}_{0.988}\text{Ge}_{0.012}$, [B] $\text{Si}_{0.957}\text{Ge}_{0.043}$, [C] $\text{Si}_{0.944}\text{Ge}_{0.056}$, [D] $\text{Si}_{0.884}\text{Ge}_{0.116}$, and [E] $\text{Si}_{0.856}\text{Ge}_{0.144}$ alloy NCs.

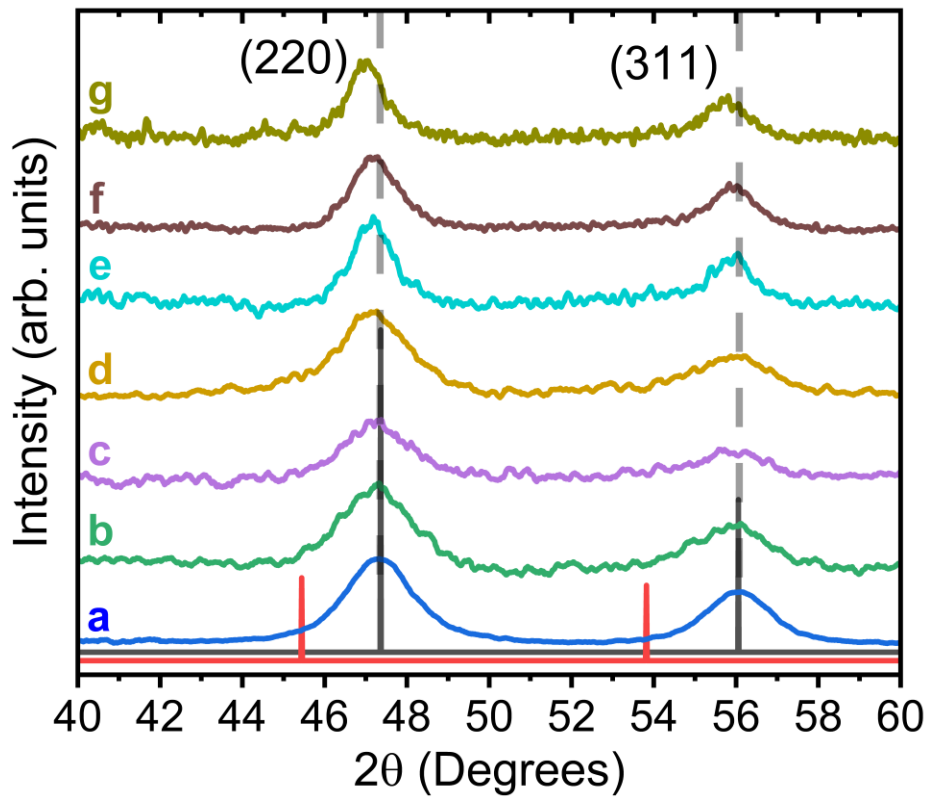


Figure S8. PXRD patterns displaying the (220) and (311) peaks of (a) $\text{Si}_{1.000}\text{Ge}_{0.000}$, (b) $\text{Si}_{0.988}\text{Ge}_{0.012}$, (c) $\text{Si}_{0.957}\text{Ge}_{0.043}$, (d) $\text{Si}_{0.944}\text{Ge}_{0.056}$, (e) $\text{Si}_{0.916}\text{Ge}_{0.084}$, (f) $\text{Si}_{0.884}\text{Ge}_{0.116}$, and (g) $\text{Si}_{0.856}\text{Ge}_{0.144}$ alloy NCs. The ICDD-PDF overlays of diamond cubic Si (JCPDS 00-001-0971) and Ge (JCPDS 01-89-5011) are shown as vertical black/dashed and red lines, respectively.

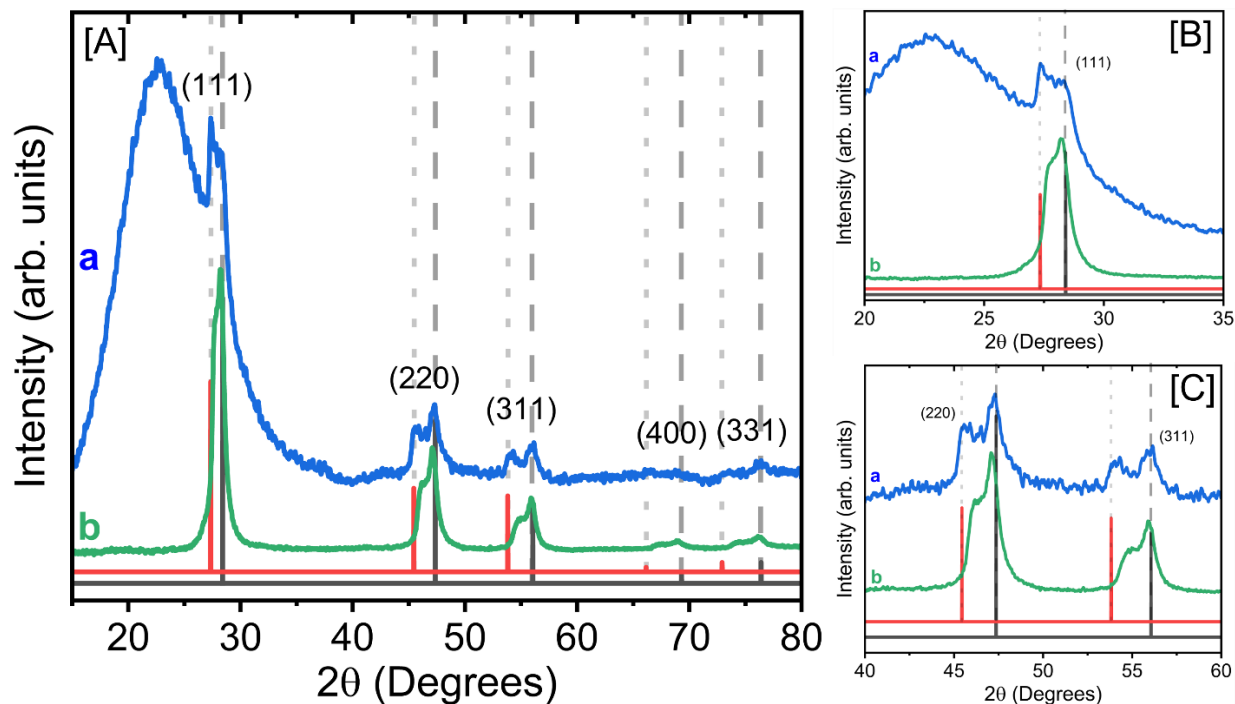


Figure S9. [A] PXRD patterns of (a) $\text{Si}_{0.920}\text{Ge}_{0.080}$ NCs (nominal composition) embedded in silica matrix prior to HF etching and (b) colloidal unstable fraction obtained after HF etching and hydrosilylation/ hydrogermylation. The large hump at $\sim 22^\circ$ corresponds to amorphous SiO_2 . [B] and [C] are zoomed in figures of [A] showing (111) and (220) peaks. The ICCD-PDF overlays of diamond cubic Si (JCPDS 00-001-0971) and Ge (JCPDS 01-89-5011) are shown as vertical black/dashed and red/dotted lines, respectively.

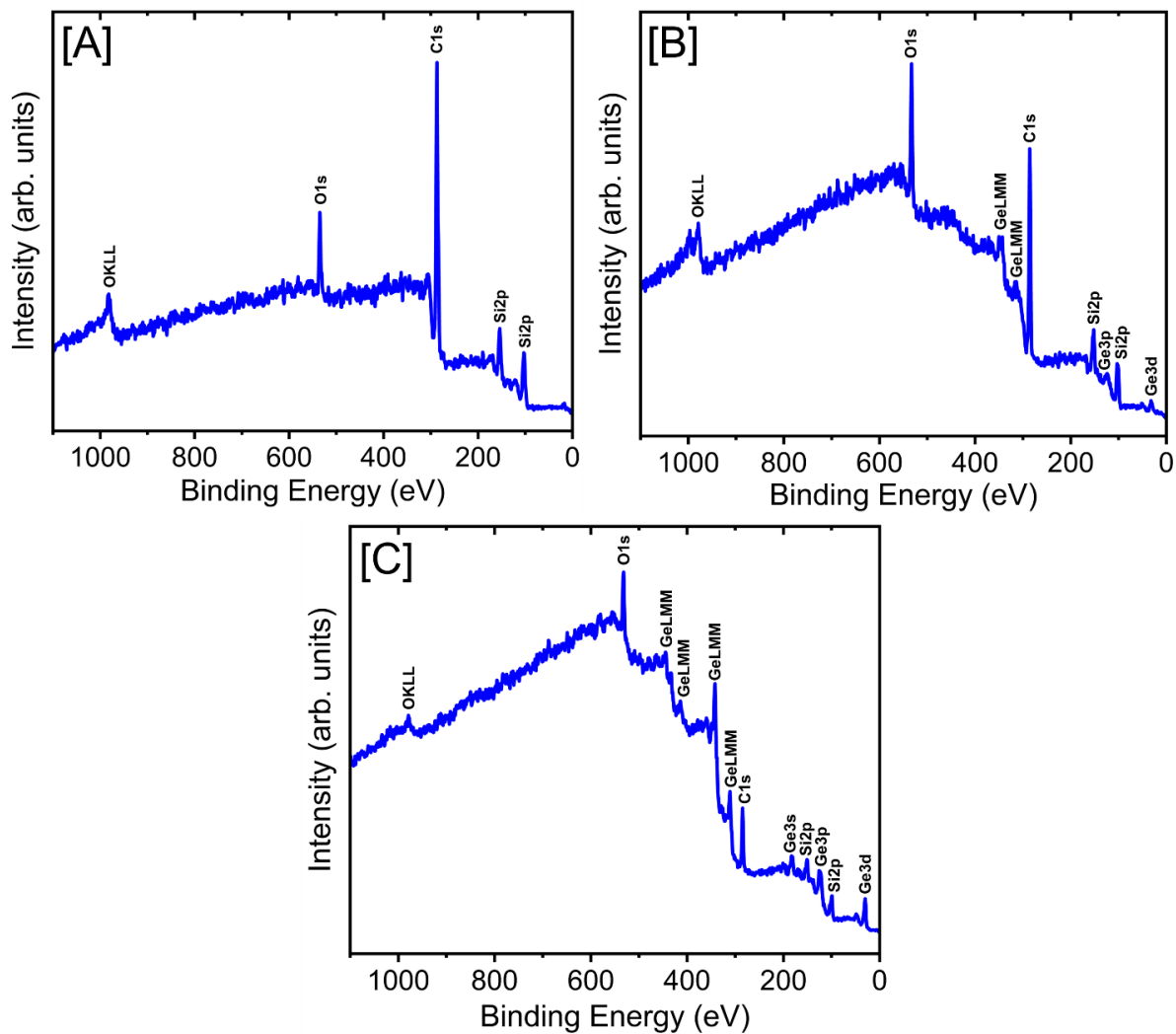


Figure S10. XPS survey scans of [A] Si, [B] Si_{0.856}Ge_{0.144} and [C] Si_{0.505}Ge_{0.495} alloy NCs.

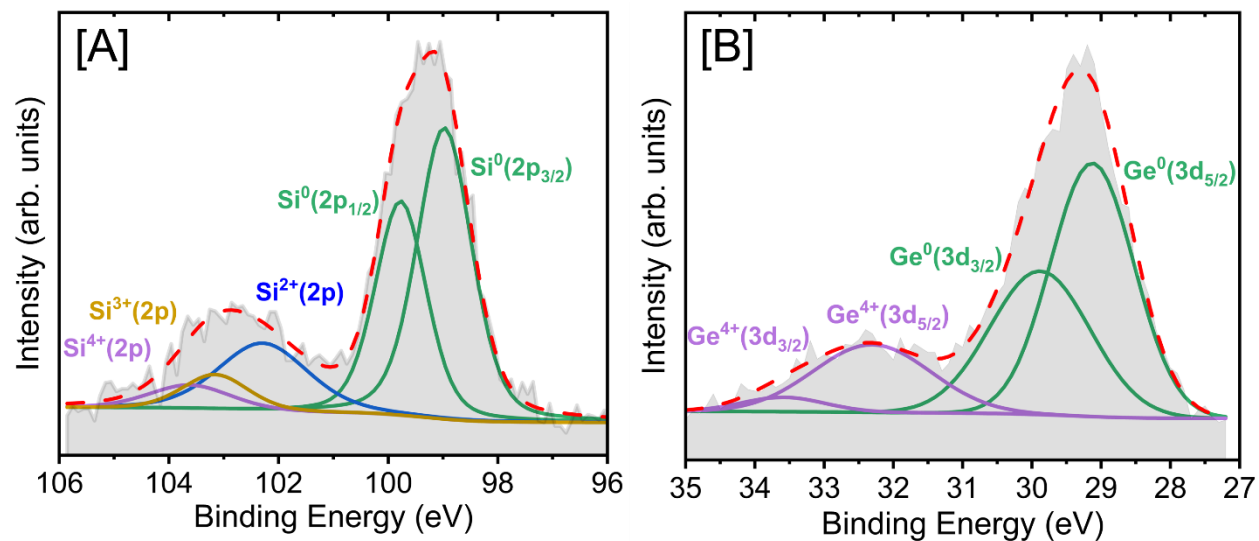


Figure S11. XPS spectra of the [A] Si 2p and [B] Ge 3d region of colloiddally unstable fraction of $\text{Si}_{0.505}\text{Ge}_{0.495}$ NCs. The shaded (semitransparent) plot represents the spectral data. The green lines represent the Si^0 and Ge^0 species whereas the blue, tan, purple, and red lines represent Si^{2+} , Si^{3+} , $\text{Si}^{4+}/\text{Ge}^{4+}$ species, and overall fitted envelope, respectively.

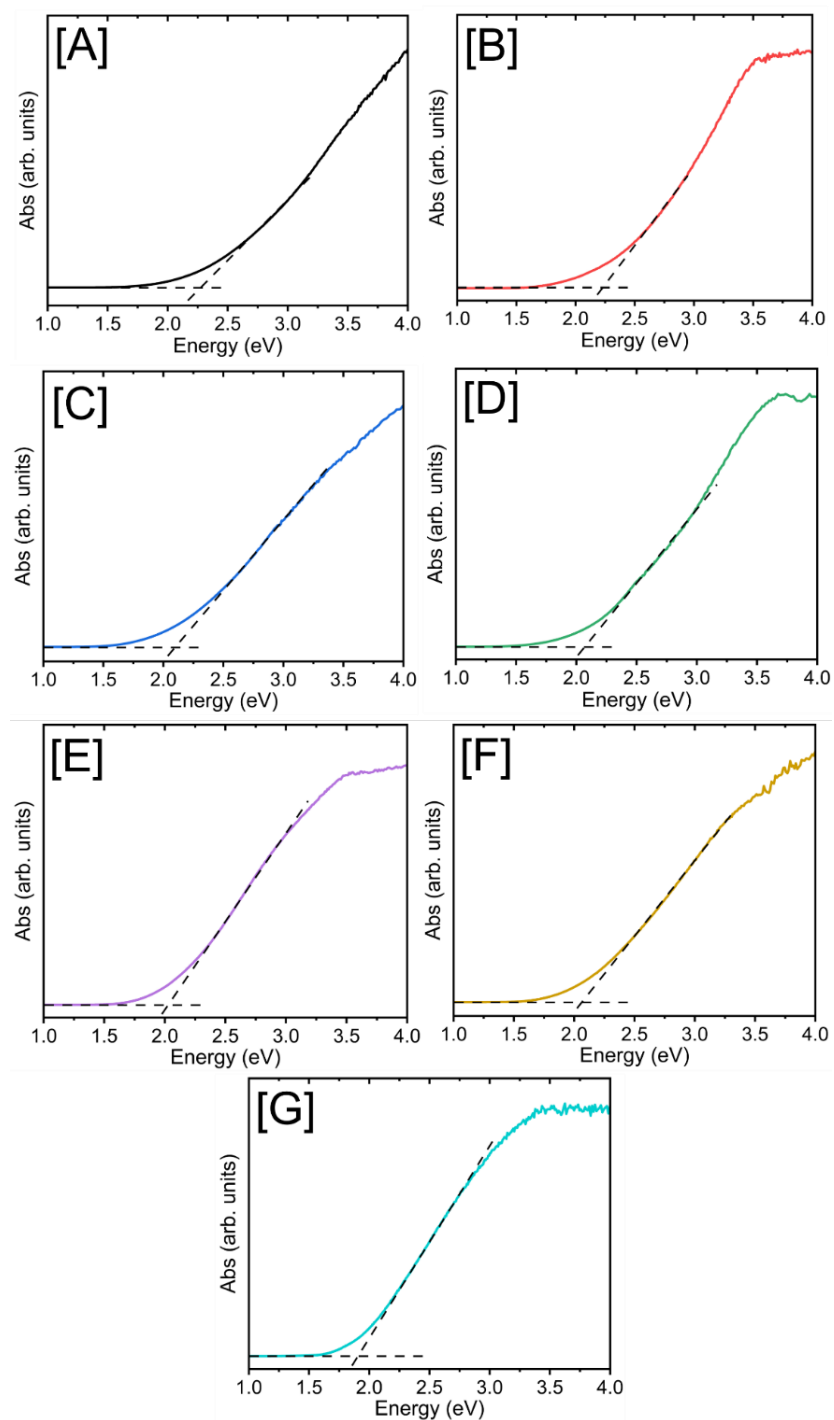


Figure S12. Solid-state diffuse reflectance spectra (converted to absorption using Kubelka-Munk remission function)¹ of (a) $\text{Si}_{1.000}\text{Ge}_{0.000}$, (b) $\text{Si}_{0.988}\text{Ge}_{0.012}$, (c) $\text{Si}_{0.957}\text{Ge}_{0.043}$, (d) $\text{Si}_{0.944}\text{Ge}_{0.056}$, (e) $\text{Si}_{0.916}\text{Ge}_{0.084}$, (f) $\text{Si}_{0.884}\text{Ge}_{0.116}$, and (g) $\text{Si}_{0.856}\text{Ge}_{0.144}$ alloy NCs. The intersection of the dashed lines correspond to the energy gap where a least-squares linear regression analysis was applied.

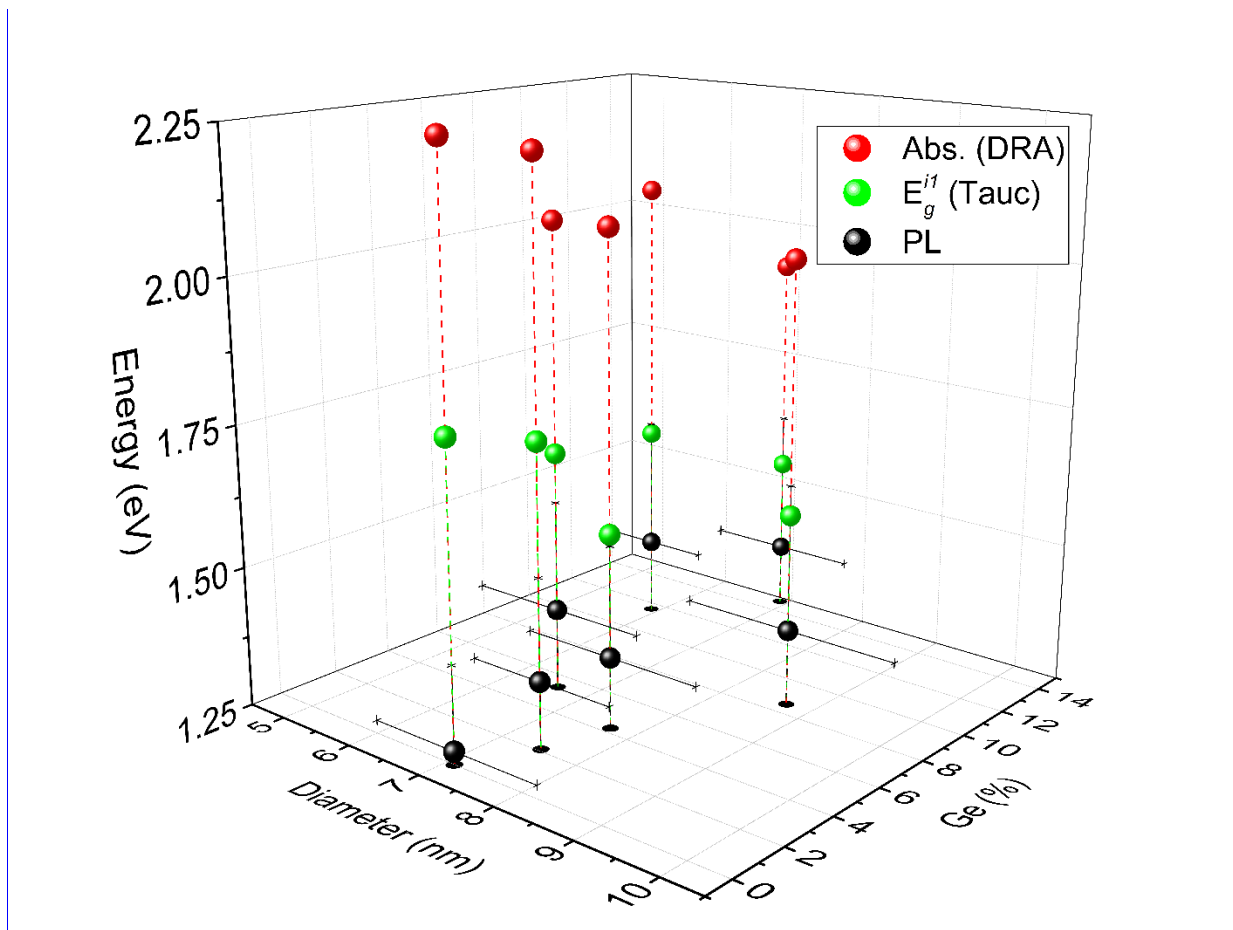


Figure S13. Energy gaps of $\text{Si}_{1-x}\text{Ge}_x$ alloy NCs obtained from absorption onsets (red), indirect Tauc analysis (green), and PL peak maxima (black) plotted against experimental NC diameters (TEM) and Ge composition (x). The full width at half maximum (FWHM) of PL peaks and NC size polydispersity are indicated by solid black error bars in the Z and X directions, respectively.

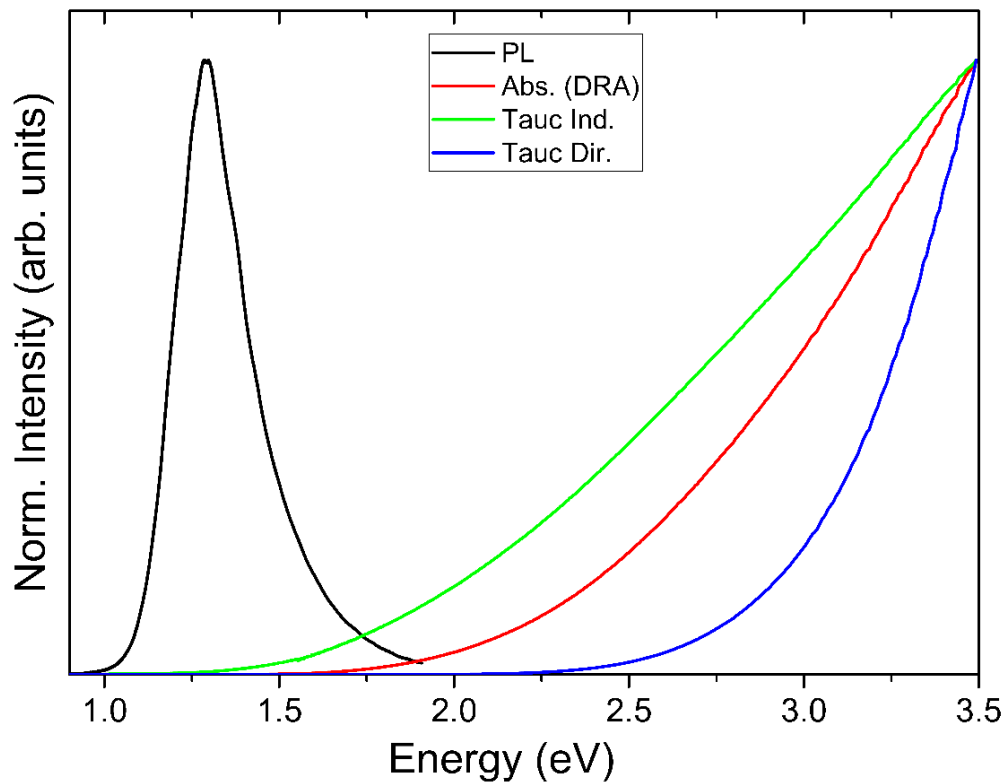


Figure S14. Solid-state PL (black) and absorption (red) spectra of 7.2 ± 0.7 nm Si NCs along with Tauc plots obtained from direct (blue) and indirect (green) gap functions.

QUANTUM YIELD MEASUREMENTS

Preliminary measurements of absolute quantum yield (QY) obtained according to the de Mello methodology² for a selection of the alloy NC samples (drop-casted on Si substrates) having Ge content $<5.6\%$ indicate an average QY of approximately 1-5%. By comparison, QY values obtained from phase pure Si NCs of various diameters produced via a similar methodology span a range of $\sim 8\text{-}30\%$,³ indicating a potential increase in the fraction of nonradiative recombination sources associated with Ge alloying; attributed to composition-related defects in other works.⁴

REFERENCES

1. A. Tsuge, Y. Uwamino, T. Ishizuka and K. Suzuki, *Appl. Spectrosc.*, 1991, **45**, 1377–1380.
2. J. C. de Mello, H. F. Wittmann, and R. H. Friend, *Adv. Mat.*, 1997, **9** (3), 230–232.
3. D. S. Pate, G. C. Spence, L. S. Graves, I. U. Arachchige and Ü. Özgür, *J. Phys. Chem. C*, 2024, **128**, 10483–10491.
4. S. Takeoka, K. Toshikiyo, M. Fujii, S. Hayashi and K. Yamamoto, *Phys. Rev. B*, 2000, **61**, 15988–15992.